SAND2018-4733J

Reactive Sputter Deposition of Pieozoelectric Sc_{0.12}Al_{0.88}N for Contour Mode Resonators

M. David Henry, Travis R. Young, Erica A. Douglas, Ben Griffin

Sandia National Labs, MESA Fabrication Facility

PO Box 5800 MS 1084, Albuquerque, New Mexico, USA 87185-1084

AVS 64th International Symposium and Exhibition, Tampa Bay, Florida, Oct. 29-Nov. 3,

2017

American Vacuum Society member.

Electronic mail: mdhenry@sandia.gov

Substitution of Al by Sc has been predicted and demonstrated to improve the piezoelectric

response in AlN with commercial market applications in radio frequency (RF) filter

technologies. Although cosputtering has achieved Sc incorporation in excess of 40%,

industrial processes requiring stable single target sputtering is currently limited. The major

concern with sputter deposition of ScAl is the control over the growth of inclusions while

simultaneously controlling film stress for suspended MEMS structures. This work

describes 12.5% ScAl single target reactive sputter deposition process, and establishes a

direct relationship between the inclusion occurrences and compressive film stress allowing

for suppression of the c-axis instability on silicon (100) and Ti/TiN/AlCu seeding layers.

An initial high film stress, for suppressing inclusions, is then balanced with a lower film

stress deposition to control total film stress to prevent Euler buckling of suspended MEMS

devices. Contour mode resonators fabricated using these films demonstrate effective

coupling coefficients up to 2.7% with figures of merit of 42. This work provides a method to establish inclusion free films in Sc substituted AlN piezoelectric films.

I. INTRODUCTION

The importance of AlN in the microelectronics industry is rapidly expanding with applications in wireless communication, ultrasonic transducers, sensors and even in multiferroics¹⁻⁴. Radio frequency (RF) filters utilizing the piezoelectric properties of the film have found large market shares with bulk acoustic wave (BAW) and surface acoustic wave (SAW) technologies⁵. And yet, even as these technologies mature new architectures for transducing an electrical signal into an acoustic resonance have emerged with contour mode resonators (CMR) utilizing the lithographic patterning of the film to define frequency response rather than film thickness⁶⁻⁸. The advantage with this technology was a wide range of achievable frequencies on the same film; approximately 1 MHz to 10 GHz⁹. This class of resonators typically utilized a Lamb wave response with electrodes placed on the top or both top and bottom of the film to extract an electromechanical coupling with the d_{31} piezoelectric coefficient¹⁰. However, this limited the electromechanical coupling coefficient (k_t²) to approximately a third of that achievable by BAW utilizing the d₃₃ piezoelectric coefficient, which severely degraded filter performance. A noteworthy exception is when a CMR has the piezoelectric thickness set such that a Lame mode can be established, in which case k_t² values can reach 6.2%¹¹.

Theoretical and experimental work have suggested that replacement of the Al in wurtzite AlN structure with Sc could boost the k_t^2 up to 5 times with a 40% Sc substitution¹²⁻¹⁴. Films of different Sc_xAl_{1-x} stoichiometry are continuing to demonstrate these realities with reactive co-sputtering deposition^{15, 16}. This work continues this technological advancement with development of reactive sputter deposition of $Sc_{0.125}Al_{0.875}N$ from a single target on silicon and AlCu seeding layers^{17, 18}. Control of deposition parameters are described with particular attention to film stress and inclusions or hillocks in the film. Recent work has suggested that these inclusions are a result of unwanted (100) growth, a so called c-axis instability in the optimal (002) wurtzite ScAlN

film and are not typically detected in rocking curves which suggest a degree of the piezoelectric mechanical coupling¹⁹. Although their work suggested inclusion prevention based on seeding from specific thin films, this work finds that control over stress conditions during deposition can greatly inhibit (100) growth in the film even on the most structural different crystal orientations such as silicon (100). Stress control over inclusions will prove critical in realization of high performance of piezoelectric CMRs in commercial RF filter applications.

II. REACTIVE SPUTTER DEPOSITION

ScAlN films were reactively sputtered using a SPTS Sigma 200 Pulsed DC Magnetron Sputtering System on low resistivity 150 mm silicon (100) wafers. The target utilized was a 300 mm target with 12.5% Sc / 87.5% Al casted using vacuum induction melting purchased from Materion. For this work, reactive sputter deposition film control techniques included variation of RF power, platen temperature and gas flow ratios between Ar and N₂. Nominal chamber conditions consisted of 5 kW of pulsed DC power, 25 sccms of Ar, 125 sccms of N₂, 100 W of RF power, with a platen temperature of 350 C. For film thickness of approximately 750 nm, a deposition time of 710 seconds was utilized.

Film characterization was performed using a TOHO laser wafer curvature for stress measurements, a Wollham ellipsometer measured index, optical loss and film thickness, and a Hitachi 4800 SEM imaged wafer surfaces at 25, 50 and 100x magnifications. The 25, 50 and 100x magnifications had field of views of approximately 17.9, 4.54, and 1.13 µm² respectively. Under SEM magnification, unusual grain formations, hillocks, were observed with typical sizes around 200 nm; in this work we denote them as inclusions in the film, Fig 1a & 1b. Fitchner et al. (2017) has described these inclusions as a c-axis instability occurring during growth in which the (100) structure becomes incorporated in the (002) wurtzite crystal¹9. TEM images demonstrate these growths begin early in film deposition and show prominently in the diffraction patterns, Fig 2. To compliment this assertion, XRD of the film was performed. In the

measurement, the (002) columnar wurtzite growth is observed at 35.9° as is a strong (100) peak at 33°, Fig 3. In previous work, it was observed that utilization of silicon baffle wafers reduced the number of inclusions but did not eliminate them¹⁸. For each of the deposition sweeps described in this work, 5 baffle wafers were utilized before the parameter sweeps occurred. This permitted the effect of the parameter being swept to control the inclusions and film performance, to be isolated from the inclusions from the baffle wafer effect.

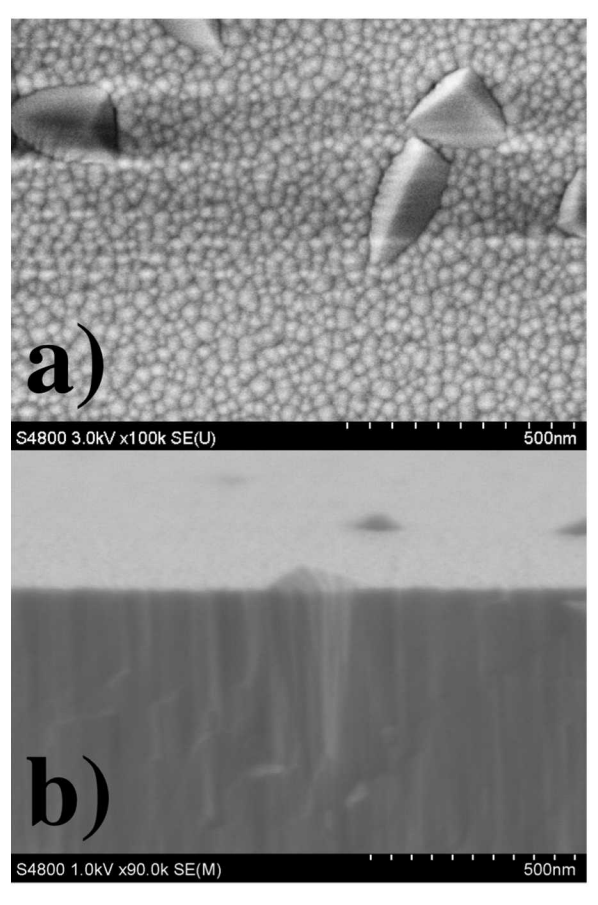


Fig 1. SEM images of deposited 750 nm thick ScAlN films. a) Top-down SEM showing c-axis oriented films with 200 nm inclusions coming thru the films. b) Cross section of film where the majority of the film is oriented along c-axis as it the inclusion.

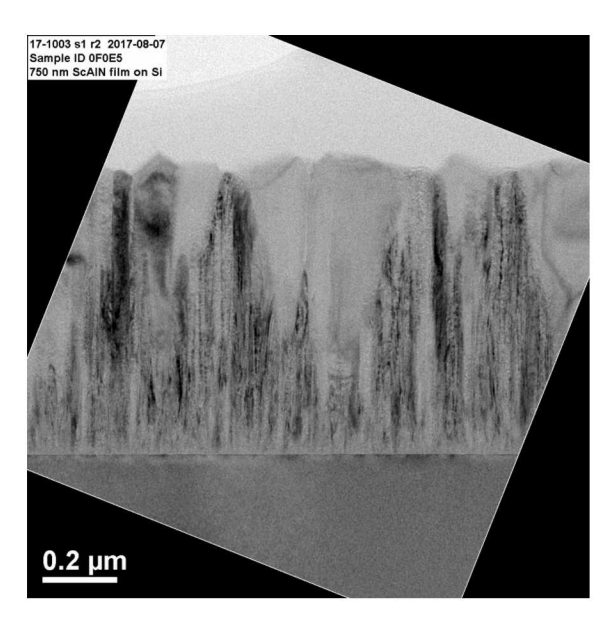


Fig 2. TEM cross section of deposited 750 nm thick ScAlN films with prominent c-axis orientation of (100) inclusions beginning around 200 nm.

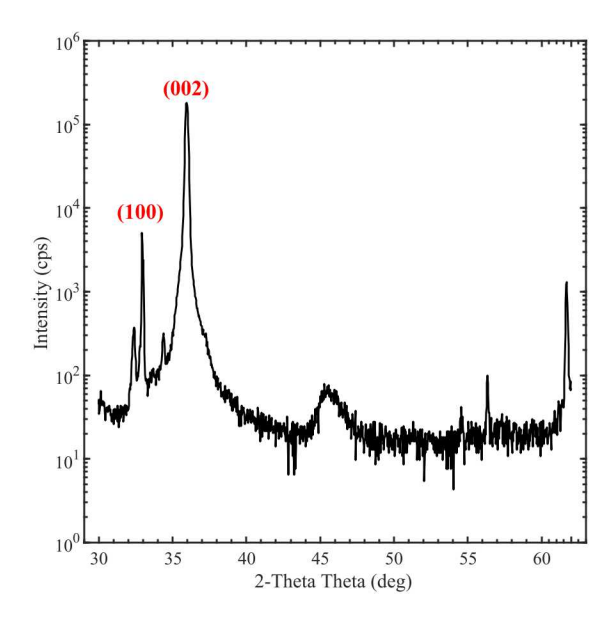


Fig 3. XRD patterning of the ScAlN film with a prominent (002) wurtzite growth at 35.9° and the inclusion (100) growth at 33°.

As is common when establishing reactively sputtered films, the platen temperature, RF sputter power, and Ar:N₂ gas ratios were varied while time was adjusted to maintain an approximate film thickness of 750 nm. Sweeping of sputter deposition parameters was towards the optimization of both film stress and reduction of inclusion numbers all while maintaining (002) orientation, Fig 4a & 4b. Increases in RF power shifted the deposited films from tensile to compressive stress as did lowering the platen

temperature also create a more compressive film. Using top down SEMs images, the number of inclusions under 50x magnification were counted at the center of the wafers. Platen temperature in the range of 350 to 400 C had minimal effect on inclusion count, but the RF power found optimum results at 100 W, and possibly higher. However, this optimal power setting placed the ScAlN film under very high compressive stress which would not be acceptable for fabrication of released structures.

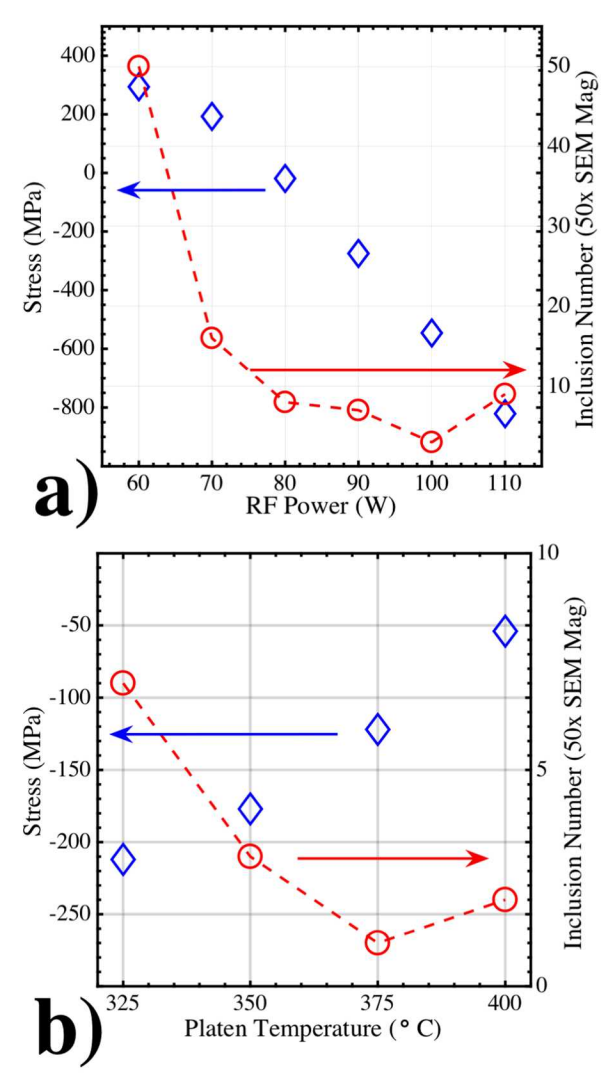


Fig 4. (Color online) Sputter deposition parameter sweep of a) RF power and b) platen temperature to optimize stress (blue diamonds) and inclusion number (red circles).

Since this process was a reactive sputtering process, the ratio of Ar to N_2 was also swept as RF power was swept. The film thickness was again kept to 750 nm. No significant change in stress or inclusion count were observed while varying gas ratios and

the trend in the films remained consistent with previous experiments' RF power effects, Fig 5a & 5b.

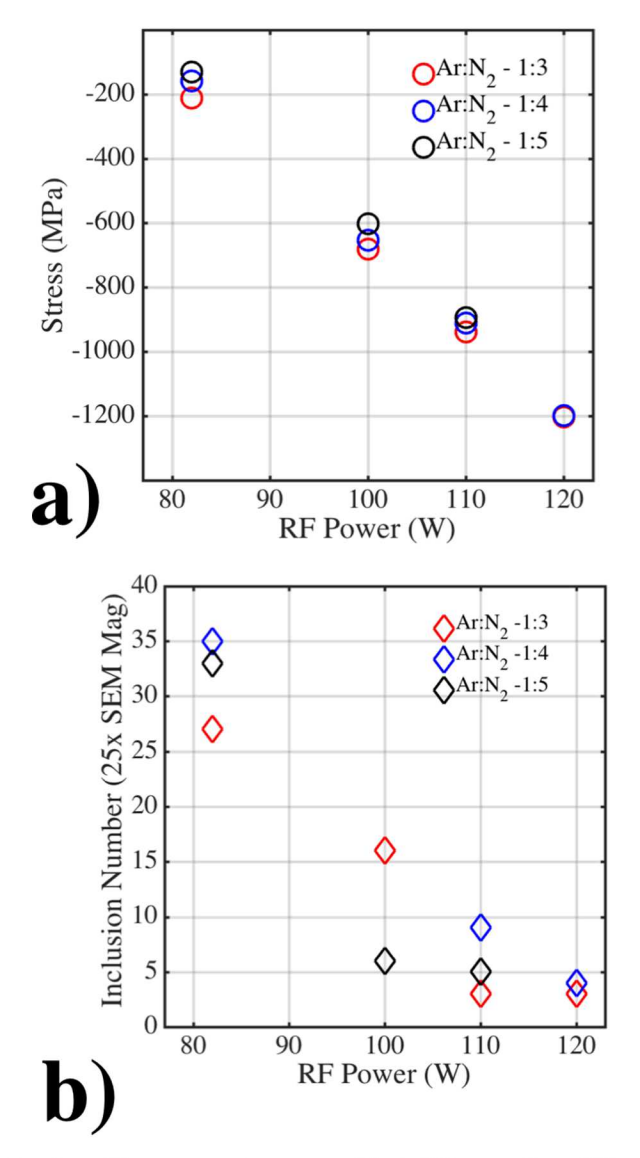


Fig 5. (Color Online) Sputter deposition parameter sweep of Ar to N2 gas ratio as RF power is swept. a) Film stress followed the same increasing compressive stress trend as seen earlier but with no significant difference with gas ratios. b) Inclusion number was observed to decrease as RF power increased, also as noted previously but with no significant difference with gas ratios.

With the power set at 100 W, a gas ratio of 1:5, and platen temperature at 375 C, XRD measured a significant suppression of the (100) peak and a highly oriented (002) ScAlN film was observed, Fig 6. Rocking curves of the films, inset Fig 6, show a 2.016° highly oriented 002 ScAlN structure. However, these films are still more than 600 MPa compressive which is not suitable for suspended devices such as CMRs.

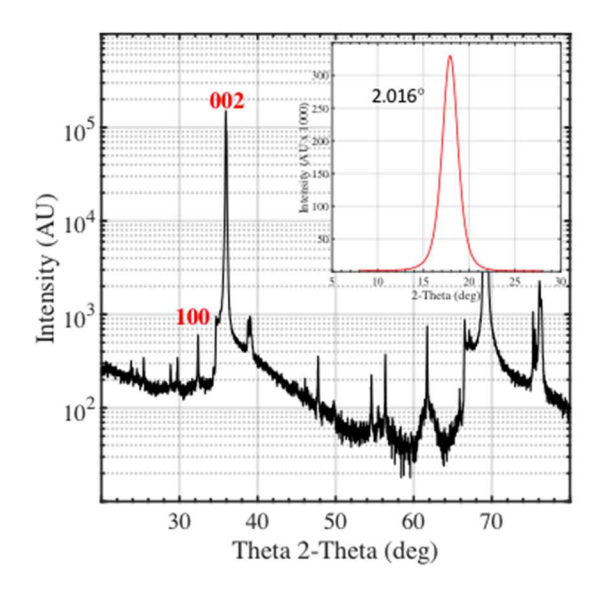


Fig 6 (Color Online) XRD patterning of the ScAlN film deposited using RF of 100W, 375 C platen temperature and gas ratio of 1:5 demonstrating a prominent (002) wurtzite growth at 35.9° and suppressed inclusion (100) growth at 33°. Inset shows a 2.016° rocking curve.

Utilizing the deposition sweeps, control over the film stress and inclusion number is observed to be predominantly controlled using RF power. To have film stress under conditions which would allow MEMS devices to be suspended, the RF power should be adjusted to lower powers such that film stress could be maintained close to zero. However, for this piezoelectric film to be free of inclusions the RF power should be shifted upwards to 100 W but would also result in a higher film stress not usable for suspended structures. This suggests then, that an initial high compressive stress at 100 W be first deposited to suppress any inclusion growth, then decreased to lower RF power to reduce the integrated film stress to levels which did not permit buckling of suspended devices. To this extent, Si wafers were again sputter deposited upon where the total sputter time was kept to 710 seconds to produce approximately 750 nm thick films, but the ratio of 100 W deposition time to 82 W deposition time was varied. For the 100 W sputtering condition, the Ar:N₂ ratio was held at 1:4 and the 82 W sputtering condition held at 1:5. The platen temperature was set to 350 C. As the deposition time ratio increased and the high compressive stress 100 W RF power condition film was thicker, the film's total stress also became both more compressive and fewer inclusions formed, Fig 7. However, a sharp drop in inclusions occurred when the ratio was 0.056; 40

seconds of the 100 W deposition condition and 670 seconds of the 82 W deposition condition.

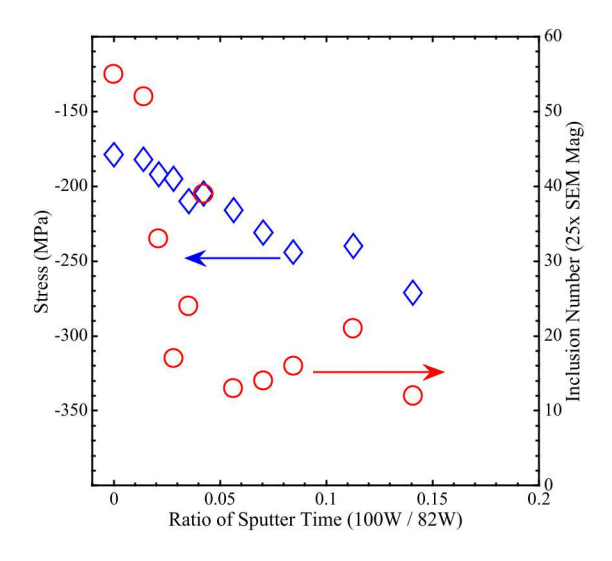


Fig 7. Film stress (diamonds) and inclusion number (circles) as ratio of sputter time for the starting high compressive stress, low inclusion 100 W RF power deposition condition to the lower compressive stress, high inclusion 82 W RF power deposition conditions. By starting film nucleation with high compressive stress, the inclusion growth could be inhibited and followed with a lower stress condition to develop films with overall low stress compatible with suspended MEMS structures.

This optimized deposition time ratio of 40:670 seconds, was then repeated at 375 C to further lower the compressive stress, and measured. As expected from Fig 4b, the film was measured to reduce the compressive stress by approximately 100 MPa. Film stress under these new conditions resulted in a film stress of -193 MPa and 5 inclusions under 25x magnification and no inclusions under 50x, Fig 8a. The film was then measured using x-ray diffraction (XRD) rocking curves to determine the piezoelectric properties, Fig 8b. The piezoelectric coupling coefficient is known to be from the wurtzite c-axis grain orientation (002) as measured using x-ray diffraction rocking curves where a higher degree of orientation suggests better coupling. This ScAlN film measured FWHM at 1.884° in the center and 1.892° at the wafer edge. With low stress, low inclusion number and rocking curves predicting good piezoelectric coupling, CMR devices should perform well when fabricated in this film.

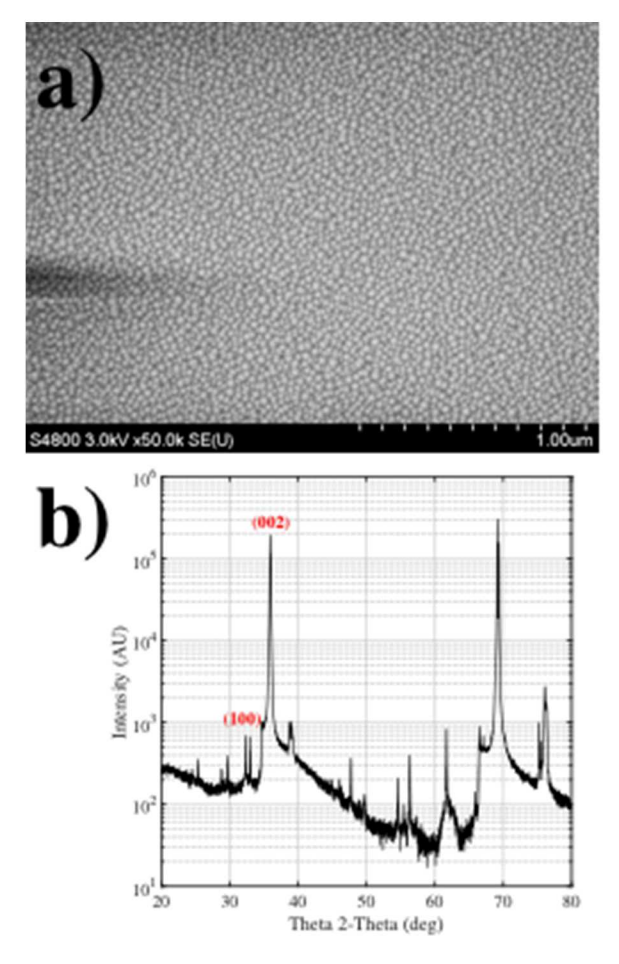


Fig 8. (Color Online) a) SEM of a 750 nm thick ScAlN film deposited utilizing a thin high compressive stress interface layer to suppress the growth of inclusions followed by a low compressive stress layer to reduce the integrated film stress. b) XRD of film showing a strong (002), c-axis orientation, with a rocking curve measurement of 1.884° and 1.892° center and edge respectively.

Although CMRs with top electrode only can achieve good quality factors and modest coupling coefficients, utilizing a bottom electrode and top electrode permits probing the full piezoelectric film^{7, 20}. The difficulty arises when attempting to orient the film on other metals¹⁹. By utilizing the technique demonstrated on silicon, we demonstrate good orientation of ScAlN on AlCu. Beginning with the deposition conditions seen on Si, an RF power sweep was performed on a sputter deposited Ti/TiN/AlCu (20/25/200 nm respectively) film stack of 100 nm of plasma enhanced tetraethylorthrosilica (PETEOS) deposited oxide. A very similar stress dependence on RF power was observed when compared with that of deposition on silicon with a shift towards being more tensile, Fig 9. Repeating the switched power sputter deposition of 40 seconds at 100 W RF power and then 660 seconds at 75 W, adjusted lower than that of the 82 W used with silicon, a film free of inclusions under all magnifications was

achieved, Fig 10a. XRD demonstrated a suppressed (100) and a rocking curve of 1.524° and 1.563° at the center and edge of the wafer respectively, Fig 10b.

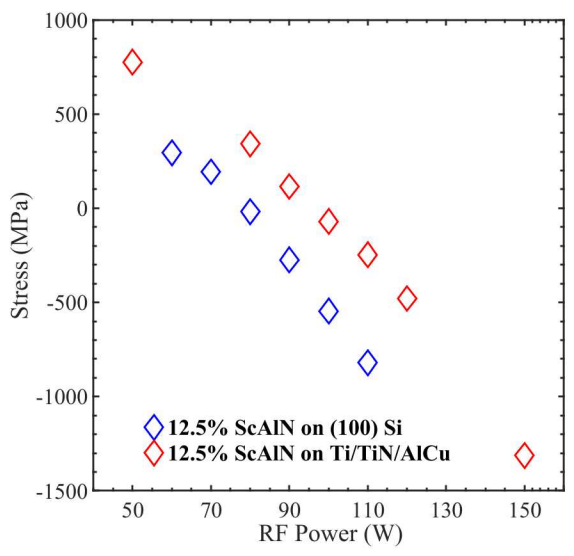


Fig 9. (Color online) Sputter deposition parameter sweep of RF power for stress control on Ti/TiN/AlCu (red) and Si (blue).

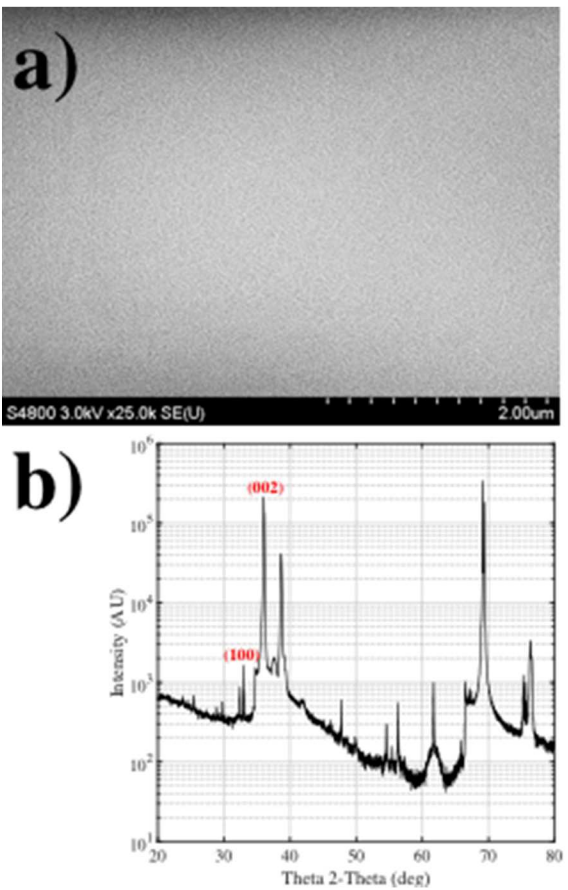


Fig 10. (Color Online) a) SEM of a 750 nm thick ScAlN film deposited on Ti/TiN/AlCu utilizing a thin high compressive stress interface layer to suppress the growth of inclusions followed by a low compressive stress layer

to reduce the integrated film stress. b) XRD of film showing a strong (002) c-axis orientation, with a rocking curve measurement of 1.524° and 1.563° center and edge respectively.

III. CMR Fabrication

Utilizing the two-step deposition process noted above, a set of CMR devices were fabricated to demonstrate this process is suitable for suspended devices over a range of frequencies, Fig 11. The deposited 756 nm film on Si was measured to have -182 MPa of stress and XRD rocking curves of 1.88° suggest the quality of the film to have good orientation and piezoelectric properties. A second wafer utilizing the Ti/TiN/AlCu metallization was also prepared using the same conditions generating the 1.528° rocking curves. The piezoelectric films then had 200 nm of Al evaporated on the surface, photoresist patterned and etched to create the IDT electrodes using an ASML stepper for the lithography and using a BCl₃/Cl₂ plasma etch chemistry in a Plasma Therm inductively coupled plasma reactive ion etcher (ICP RIE). A second lithographic step was utilized to establish the edge of the resonator and open the ScAlN film to expose the silicon release pit. Again, photoresist was used and the piezoelectric film etched in BCl₃/Cl₂ plasma etch chemistry. Finally, a XeF₂ isotropic etch was used to remove the silicon substrate under the CMR and suspend the devices¹⁸.

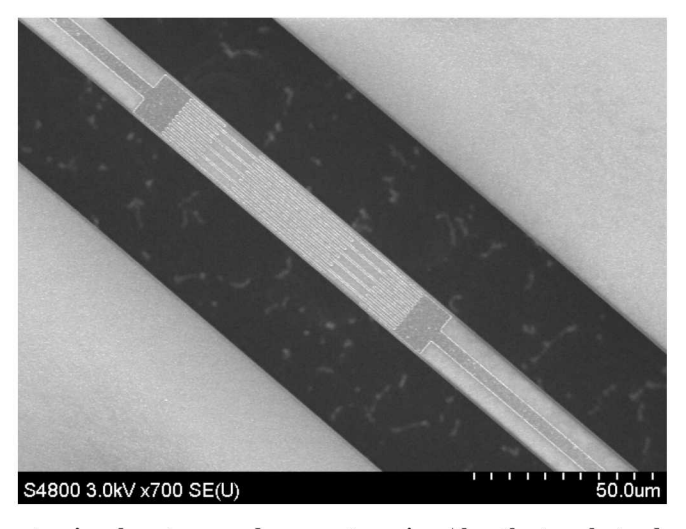


Fig 11. SEM of a width extensional contour mode resonator using Al as the top electrode on 750 nm thick ScAlN. The silicon under the ScAlN film was etched away using XeF_2 to suspend the device.

Devices were electrically tested using a Keysight RF network analyzer and ground-signal-ground (GSG) RF probes. Tested devices spanned a frequency range of 500 MHz to 2 GHz with each transmission, S₁₂, sweep consisting of 1601 points. Two representative devices with designed wavelengths of 10.6 µm and 9.6 µm were selected for each wafer from the same die, from the wafers' center and the S₁₂ vs. frequency plotted, Fig 12. Addition of the bottom electrode had multiple significant effects on device performance. First the acoustic velocity decreased from approximately 9800 m/sec to 8400 m/sec. Second, the baseline insertion loss increased from -35 dB to -20 dB likely due to capacitive shunting and the low resistance bottom metal layer. Finally, CMR performance significantly improved from due to the increased electric field interaction thru the piezoelectric film. Using the Butterworth Van-Dyke (BVD) model, extraction of the effective electromechanical coupling coefficient and the unloaded quality factor could be made for the devices displayed, Table I^{18,21}.

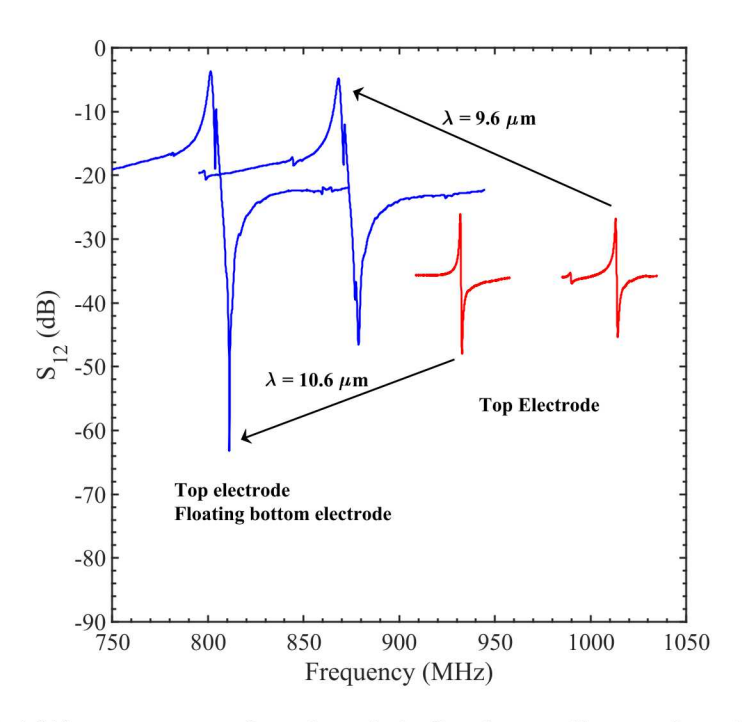


Fig 12. (Color online) S12 measurements of top electrode (red) and top and bottom electrode (blue) CMRs for designed 10.6 and 9.6 μ m wavelengths.

TABLE I. CMR DEVICE PERFORMANCE.

		Series	Unloaded		FOM
Wavelength		Resonance	Quality	k_{eff}^2	
(∞m)	CMR metal	(MHz)	Factor	(%)	
9.6	Тор	1014.1	1147	0.2033	2.34
10.6	Top	931.9	1669	0.1942	3.25
9.6	Top/Bottom	868.2	1520	2.3894	37.21
10.6	Top/Bottom	801.4	1491	2.7525	42.20

IV. CONCLUSIONS

This work has described a single target sputter deposition process for highly oriented (002) wurtzite Sc_{0.125}Al_{0.875}N, 750 nm thick films on (100) silicon substrates seeded on both silicon and Ti/TiN/AlCu layers. Stress control over the deposition was observed to be significantly controlled used the RF sputter power with some modulation due to platen temperature. Furthermore, the c-axis instability where (100) inclusions begin to grow in the (002) film, were also suppressed by placing the sputtered film under significant amount of compressive stress initially then continuing the deposition under lower RF power conditions. The second power permitted the total film stress to be adjusted such that suspended devices could avoid buckling conditions.

Suspended CMR devices fabricated on both silicon seeded and AlCu seeded ScAlN films. Rocking curve measurements placed these films with 1.884° and 1.524° FWHM suggesting a highly oriented piezoelectric film. Representative devices were fabricated on both substrates with unloaded Q's of approximately 1500 and k²_{eff} up to 0.2% and 2.7% for silicon and AlCu seeded devices respectively. Established FOM up to 42 were demonstrated suggesting that indeed, high performing CMR devices could be realized using increased Sc concentration.

ACKNOWLEDGMENTS

This project was supported by the LDRD program at Sandia National Laboratories. Sandia National Laboratories is a multi-mission laboratory managed and operated by National Technology and Engineering Solutions of Sandia, LLC., a wholly owned subsidiary of Honeywell International, Inc., for the U.S. Department of Energy's National Nuclear Security Administration under contract DE-NA-0003525. The authors acknowledge and thank the staff of Sandia's MESA fabrication facility.

The authors acknowledge and thank the staff of Sandia's MESA fabrication facility and the work of Robert Timon.

- 1. C. D. Nordquist, D. W. Branch, T. Pluym, S. Choi, J. H. Nguyen, A. Grine, C. W. Dyck, S. M. Scott, M. N. Sing and R. H. Olsson III, Journal of Micromechanics and Microengineering **26** (10), 104001 (2016).
- 2. C. D. Nordquist, M. D. Henry, J. H. Nguyen, P. Clews, S. Lepkowski, A. Grine, C. W. Dyck and R. H. Olsson, presented at the Microwave Symposium (IMS), 2016 IEEE MTT-S International, 2016 (unpublished).
- 3. T. Nan, Y. Hui, M. Rinaldi and N. X. Sun, Scientific reports 3 (2013).
- 4. D. A. Horsley, R. J. Przybyla, M. H. Kline, S. E. Shelton, A. Guedes, O. Izyumin and B. E. Boser, presented at the Micro Electro Mechanical Systems (MEMS), 2016 IEEE 29th International Conference on, 2016 (unpublished).
- 5. K.-y. Hashimoto, in *Piezoelectric MEMS Resonators* (Springer, 2017), pp. 203-220.
- 6. M. Rinaldi, in *Piezoelectric MEMS Resonators* (Springer, 2017), pp. 175-202.
- 7. G. Piazza, P. J. Stephanou and A. P. Pisano, Journal of Microelectromechanical Systems **15** (6) (2006).
- 8. G. Piazza, in *Resonant MEMS* (Wiley-VCH Verlag GmbH & Co. KGaA, 2015), pp. 147-172.
- 9. C. D. Nordquist and R. H. Olsson, in *Wiley Encyclopedia of Electrical and Electronics Engineering* (John Wiley & Sons, Inc., 2014).
- 10. B. A. Auld, Acoustic fields and waves in solids. (R.E. Krieger, 1990).
- 11. C. Cassella, G. Chen, Z. Qian, G. Hummel and M. Rinaldi, presented at the Proc. Solid-State Sens., Actuators Microsyst. Workshop (Hilton Head), 2016 (unpublished).
- 12. P. Muralt, in *Piezoelectric MEMS Resonators* (Springer, 2017), pp. 3-37.
- 13. A. Teshigahara, K.-y. Hashimoto and M. Akiyama, presented at the Ultrasonics Symposium (IUS), 2012 IEEE International, 2012 (unpublished).
- 14. M. Akiyama, K. Kano and A. Teshigahara, Applied Physics Letters **95** (16), 162107 (2009).
- 15. J. Tang, D. Niu, Z. Tai and X. Hu, Journal of Materials Science: Materials in Electronics **28** (7), 5512-5517 (2017).
- 16. M. Akiyama, T. Kamohara, K. Kano, A. Teshigahara, Y. Takeuchi and N. Kawahara, Advanced Materials **21** (5), 593-596 (2009).
- 17. K. Umeda, H. Kawai, A. Honda, M. Akiyama, T. Kato and T. Fukura, presented at the Micro Electro Mechanical Systems (MEMS), 2013 IEEE 26th International Conference on, 2013 (unpublished).
- 18. M. D. Henry, R. Timon, T. R. Young, C. Nordquist and B. Griffin, ECS Transactions 77 (6), 23-32 (2017).

- 19. S. Fichtner, N. Wolff, G. Krishnamurthy, A. Petraru, S. Bohse, F. Lofink, S. Chemnitz, H. Kohlstedt, L. Kienle and B. Wagner, Journal of Applied Physics **122** (3), 035301 (2017).
- 20. V. Yantchev and I. Katardjiev, Journal of Micromechanics and Microengineering **23** (4), 043001 (2013).
- 21. R. Abdolvand, H. Fatemi and S. Moradian, in *Piezoelectric MEMS Resonators* (Springer, 2017), pp. 133-152.